Bulgarian Chemical Communications, Volume 46, Number 3 (pp. 645– 651) 2014

Qualitative investigation of the convective boiling heat transfer of dilute Al_2O_3-water/glycerol solution inside the vertical annuli

M. M. Sarafraz*, F. Hormozi

Faculty of Chemical, Petroleum and Gas Engineering, Semnan University, Semnan, Iran

Received July 18, 2013; Revised February 22, 2014

In this work, the flow boiling heat transfer coefficient of Al_2O_3-water/glycerol nanofluids was experimentally investigated under different operating conditions. The influence of different operating parameters such as heat flux, mass flux and sub-cooling temperature, as well as concentration of nanofluids on the convective boiling heat transfer coefficient was studied and discussed. The results demonstrated that two heat transfer regions with different heat transfer mechanisms can be distinguished during the convective boiling of nanofluids, namely single-phase forced convection and two-phase nucleate boiling. The results also showed that with increasing the heat and mass fluxes, the heat transfer coefficient of nanofluid increases and with increasing the nanofluid concentration, the heat transfer coefficient decreases which is due to the deposition of nanoparticles on the heater surface. The sub-cooling temperature only influences the onset of nucleate boiling.

Keywords: Al_2O_3, water/glycerol, nanoparticles, forced convection, nucleate boiling

INTRODUCTION

Boiling and two-phase flow phenomena are used in a variety of industrial processes and applications, such as refrigeration, air-conditioning and heat pumping systems, energy conversion systems, heat exchange systems, chemical thermal processes, cooling of high-power electronic components, cooling of nuclear reactors, micro-fabricated fluidic systems, thermal processes in aerospace stations and bioengineering reactors [1]. In nuclear power applications, boiling heat transfer plays a key role both in the efficient energy transportation during the normal operation and in the successful decay heat removal for the transient accident condition, due to the large latent heat of water and the bubble-driven convection or turbulence. Specifically, to prevent the core melt down and to mitigate the leakage of radioactivity to the outside of the reactor vessel, successful removal of decay heat is necessary [2]. Solid particles of nominal size 1–100 nm are called nanoparticles, and low-concentration dispersions of such particles in a base fluid are called nanofluids. Nanofluids are known to display a significant increase in thermal conductivity over that of the base fluid [3-7]. Early studies on the utilization of nanofluids in flow and pool boiling have mainly focused on the critical heat flux and surface characteristics of a heating section, as well as on the thermal conductivity enhancement and the parameters that govern this behavior [8-17]. One may want some more information about the recent flow boiling heat transfer research [18-22]. In previous studies, most investigators pay more attention to the critical heat flux and surface characteristics of the heating sections. Less attention has been paid to the forced convective and flow boiling heat transfer coefficient of the nanofluid due to the undesirable deterioration of the heat transfer coefficient.

The purpose of this study is to experimentally measure the forced and nucleate flow boiling heat transfer coefficient of Al_2O_3-water/glycerol nanofluid and investigate the influence of different operating conditions such as heat flux, flow rate and volumetric concentrations of the test nanofluid as well as sub-cooling temperature on the single phase and two-phase flow-boiling of the Al_2O_3-water/glycerol nanofluid.

EXPERIMENTAL

Different volumetric concentrations of nanofluids were prepared using two-step methods. The Al_2O_3 nanoparticles (45-50 nm, PlasmaChem GmbH, Germany) were uniformly dispersed into the base fluid (70 vol % of water and 30 vol % of glycerol) to obtain a stable nanofluid. In the present work, deionized water was considered as the base fluid. Briefly, the preparation steps were:

* To whom all correspondence should be sent:
E-mail: mohamadmohsensarafraz@gmail.com

I. The mass of Al_2O_3 was weighed on a digital electronic balance (A&D EK Series Portable Balances, EK-1200i).

II. The weighed Al_2O_3 nanoparticles were added to the weighed water/glycerol mixture while it was agitated in a flask (using a magnetic motorized stirrer (Hanna instruments Co.) Also, 0. 1 vol. % of QF-STK190 dispersant was added to the nanofluid as a stabilizer. Experiments were carried out on the nanofluids to check their stability and dispersion. Dynamic light scattering (DLS) test was also done (using a Malvern DLS device) to check the nanoparticle size count.

III. UP400S ultrasonic Hielscher GmbH (400W / 24 kHz) was used to uniformly disperse the nanoparticles into the water/glycerol mixture.

In the present work, nanofluids with volumetric concentrations of 0.5%, 1% and 1.5% were prepared using 45-50 nm (claimed by manufacturer) Al_2O_3 nanoparticles and water/glycerol 70:30 base fluid. Particle size measurements and XRD test of the solid particles were performed to check the size and quality of nanoparticles. As can be seen in Fig.1, maximum size count corresponds to 45-50 nm nanoparticles.

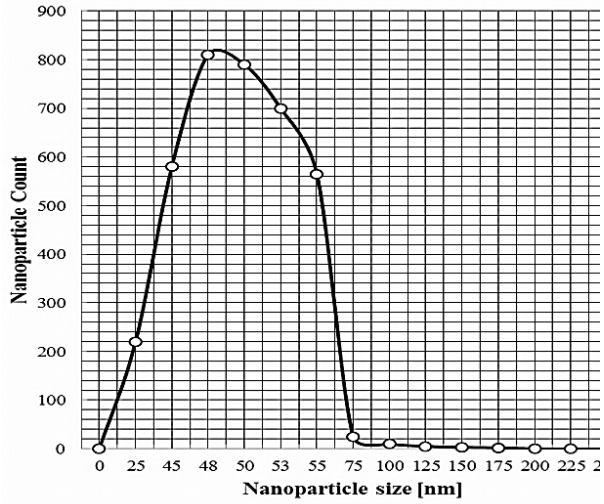

Fig. 1. Particle size distribution of Al_2O_3 nanoparticles

Fig. 2 depicts the TEM image of the Al_2O_3 nanoparticles. This image shows that particles are well dispersed in water/glycerol and there is no agglomeration and clustering inside the nanofluid. The XRD pattern (Fig. 3) depicts a single-phase Al_2O_3 with a monoclinic structure. No significant peaks of impurities are found in the XRD pattern. The peaks are broad due to the nano-size effect. The scheme of the experimental close loop is shown in Fig. 4. The working fluid enters the loop from a main tank through the isolated pipes and is continuously circulated by a centrifugal pump (DAB Co.). Due to the importance of the fluid flow rate in flow boiling heat transfer, a Netflix® ultrasonic flow meter was also installed in the fluid line to measure the flow rate. The fluid temperature was measured by two PT-100 thermometers installed in two thermo-wells located just before and after the annular section. Resistance thermometers or PT, also called resistance temperature detectors (RTDs), are the sensors used to measure the temperature by correlating the resistance of the RTD element with temperature. Most RTD elements consist of a fine coiled wire wrapped around a ceramic or glass core. This type of thermocouple is shown as PT-100. The complete cylinder was made from stainless steel 316a. Thermometer voltages, current and voltage drop from the test heater were all measured and processed with a data acquisition system in conjunction with a proportional-integral-differentiate (PID) temperature controller. The test section shown in Fig. 4 consists of an electrically heated cylindrical DC bolt heater (manufactured by Cetal Co.) with a stainless steel surface, mounted concentrically within the surrounding pipe. The

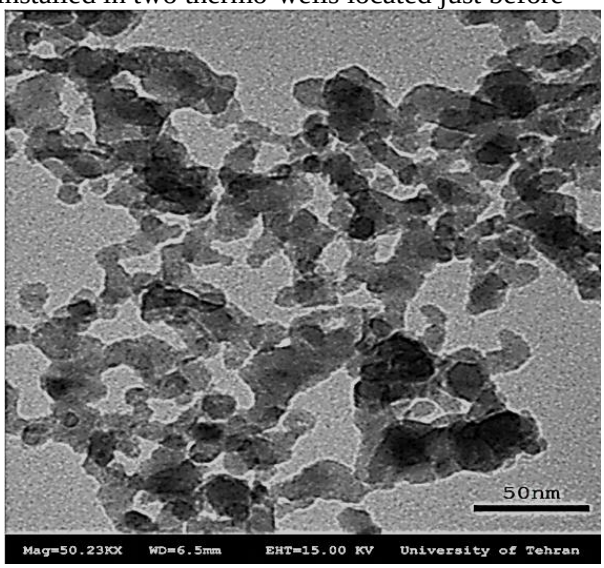

Fig. 2. TEM image of Al_2O_3 nanofluid; vol. %=1.5

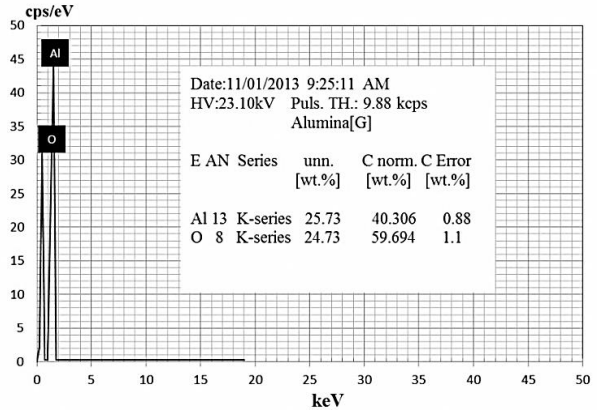

Fig. 3. XRD results of Al_2O_3 solid nanoparticles

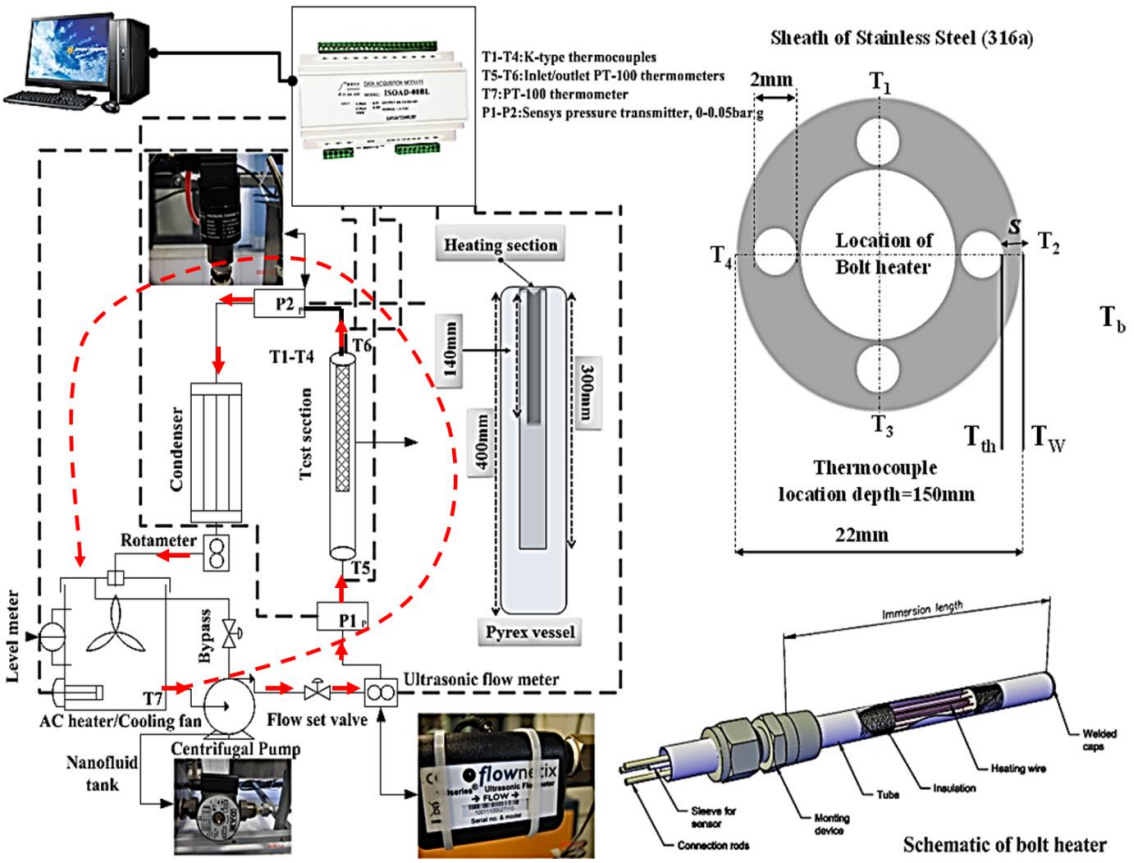

Fig. 4. Scheme of the test loop

dimensions of the test section are: diameter of heating rod 22 mm; annular gap diameter (hydraulic diameter) 30 mm; length of the pyrex tube 400 mm; length of stainless steel rod 300 mm; length of heated section 140 mm which means that just the first 140 mm of stainless steel are heated uniformly and radially by the heater. The axial heat transfer through the rod can be ignored because of the insulation of both ends of the heater. The heat flux and wall temperature can be as high as 190,000 W m^{-2} and 163°C, respectively. The local wall temperatures were measured with four stainless steel sheathed K-type thermocouples installed close to the heat transfer surface. The temperature drop between the thermocouples location and the heat transfer surface can be calculated from:

$$T_w = T_{th} - \dot{q}\frac{s}{\lambda_w} \tag{1}$$

The ratio between the distance of the thermometers from the surface and the thermal conductivity of the tube material (s/λ_w) was determined for each K-type thermocouple by calibration using the Wilson plot technique [23]. The average temperature difference for each test section was the arithmetic average of the four thermometers readings around the rod circumference. The average of 10 voltage readings was used to determine the difference between the wall and bulk temperature for each thermometer. All K-type thermocouples were thoroughly calibrated using a constant temperature water bath, and their accuracy was estimated to ±0.3K. The local heat transfer coefficient α was then calculated from:

$$\alpha = \frac{\dot{q}}{(T_w - T_b)_{ave.}} \tag{2}$$

To minimize the thermal contact resistance and temperature jump, high-quality silicone paste was injected into the thermocouple locations and also on the heater wall to expel the possible air from the center of the heating section and around the heater. To avoid possible heat loss, the main tank circumferences were heavily insulated using industrial glass wool. To control the fluctuations due to alternative current, a regular DC power supply was employed to supply the needed voltage to the central heater. Likewise, to visualize the flow and boiling phenomenon, the annulus was made of Pyrex glass.

The uncertainties of the experimental results were analyzed by the procedures proposed by Kline and McClintock [24]. The method is based on careful specification of the uncertainties in the various primary experimental measurements. The

heat transfer coefficient can be obtained using Eq. (3):

$$\alpha = \frac{\rho V C_{pnf} (T_{out} - T_{in})}{(T_w - T_b)_{av.}} \quad (3)$$

As seen from Eq. (3), the uncertainty in the measurement of the heat transfer coefficient can be related to the errors in the measurements of volume flow rate, hydraulic diameter, and all temperatures, as follows:

$$\alpha = f\ \{V, A_h, (T_{out} - T_{in}), (T_w - T_b)\} \quad (4)$$

$$\partial\alpha = \sqrt{\left[\left(\frac{\partial\alpha}{\partial V}\right).\delta V\right]^2 + \left[\left(\frac{\partial\alpha}{\partial A}\right).\delta A\right]^2 + \left[\left(\frac{\partial\alpha}{\partial(\mathrm{Tout} - \mathrm{Tin})}\right).\delta(\mathrm{Tout} - \mathrm{Tin})\right]^2 + \left[\left(\frac{\partial\alpha}{\partial(\mathrm{Tw} - \mathrm{Tb})}\right).\delta(\mathrm{Tw} - \mathrm{Tb})\right]^2} \quad (5)$$

According to the above uncertainty analysis, the uncertainty in the measurement of the heat transfer coefficient was found to be 16.23%. The uncertainty of the equipment is presented in Table 1. The main source of uncertainty is the temperature measurement and its related devices.

Table 1. Summary of the uncertainty analysis

Parameter	Uncertainty
Length, width and thickness, (m)	$\pm 5\times10^{-5}$
Temperature, (K)	±0.3K
Water flow rate, (l. min^{-1})	±1.5% of readings
Voltage, (V)	±1% of readings
Current, (A)	±0.02% of readings
Cylinder side area, (m^2)	$\pm 4\times10^{-8}$
Flow boiling heat transfer coefficient, (W/m^2.K)	±16.23 **%**

RESULTS AND DISCUSSION

In this section, the effect of different operating parameters on the flow boiling heat transfer coefficient of Al_2O_3-water/glycerol is briefly discussed.

Effect of heat flux

The experimental results demonstrated that the heat transfer coefficient in both heat transfer regions is a direct function of the heat flux. On increasing the heat flux, the heat transfer coefficient of the nanofluid in both the forced convective and the nucleate boiling heat transfer regions significantly increases due to the increased number of nucleation active sites on the heater surface. On the other hand, on increasing the heat flux, the rate of bubble formation dramatically increases. Fig. 5 presents the influence of the heat flux on the convective boiling heat transfer of the Al_2O_3-water/glycerol solution. Fig. 6 depicts the effect of heat flux on bubble formation of nanofluids.

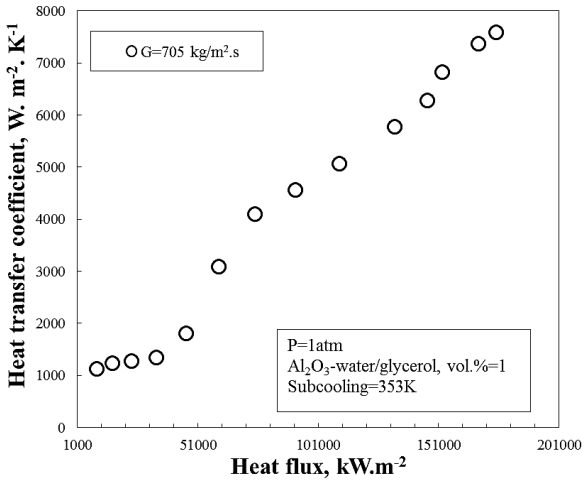

Fig. 5. Effect of heat flux on the flow boiling heat transfer coefficient of the Al_2O_3-water/glycerol nanofluid

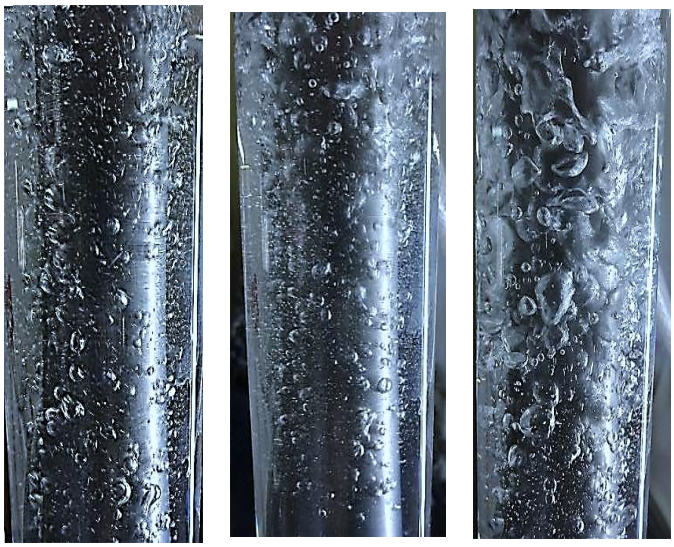

a) Heat flux 34kW/m^2 b) Heat flux 59kW/m^2 c) Heat flux 115kW/m^2

Fig. 6. Bubble formation in flow boiling heat transfer of the Al_2O_3-water/glycerol nanofluid

Effect of mass flux of fluid

Fluid flow rate (volumetric flux or mass flux) has a strong influence on the flow boiling heat transfer coefficient in both heat transfer regions. Experimental results showed that the heat transfer coefficient significantly increases when the fluid mass flux increases.

Fig. 7 presents the effect of fluid flow rate on the flow boiling heat transfer coefficient of Al_2O_3-water/glycerol nanofluids.

Effect of concentrations

The effect of concentration of nanofluids on the heat transfer coefficient in flow boiling of Al_2O_3-

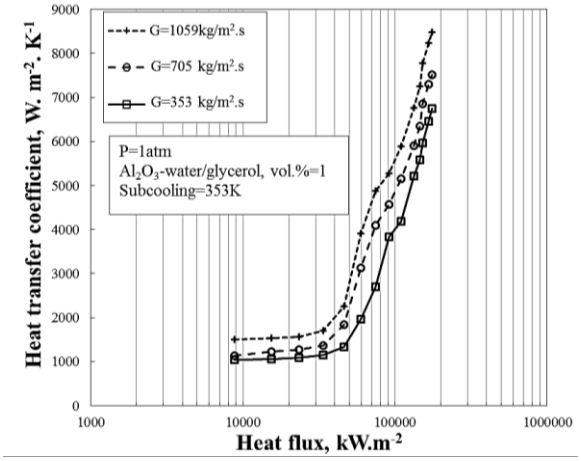

Fig. 7. Effect of mass flux on the heat transfer coefficient of the Al_2O_3-water/glycerol nanofluid

water/glycerol is represented in this section. As can be seen from figures 9 and 10, when the concentration of nanofluids increases, in the forced convective region the heat transfer coefficients increase, while for the nucleate boiling region, the heat transfer coefficients deteriorate. Due to the sedimentation of nanoparticles around the heating section and scales created on the surface, the surface heat transfer resistance increases and the surface becomes isolated against the heat transfer. Moreover, the surface characteristics significantly change and the surface wettability would also be affected by deposition, more bubbles covering the heating surface would lead the heat transfer to decrease. Fig. 8 illustrates the influence of concentration of nanofluids on the flow boiling heat transfer coefficient. For better understanding, the surface roughness was determined before and after the experiments. To this purpose the profile meter Elcometer-7061-MarSurf PS1 surface roughness tester was employed with uncertainty of ± 0.2. According to roughness meter results, the surface roughness due to the presence of nanoparticles has significantly increased.

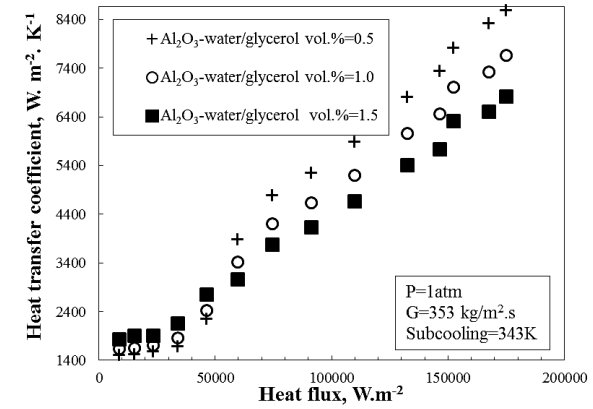

Fig. 8. Influence of the concentration of nanofluid on the flow boiling heat transfer coefficient

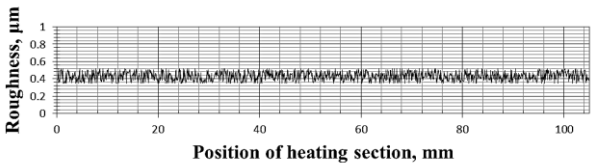

Fig. 9 Roughness of the heating section before scale formation on the surface

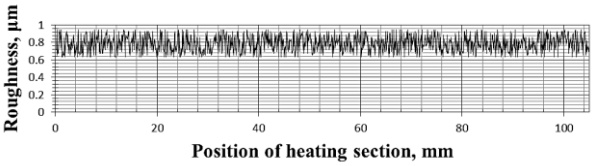

Fig. 10 Roughness of surface after the experiments; vol. %=1.5

Effect of sub-cooling temperature

Influence of the sub-cooling temperature can only be seen on the onset of nucleate boiling (ONB) point. In fact, ONB is the boundary separating the forced convective and the nucleate boiling heat transfer regions. However, the first bubble may be seen at this point or even not be seen by naked eyes. Briefly speaking, with increasing the sub-cooling temperature of the fluid, the heat flux corresponding to the ONB point significantly decreases. A small increase in the heat transfer coefficient in the nucleate boiling region is reported while no significant influence on the forced convective heat transfer coefficient is seen. Fig. 11 presents the influence of sub-cooling temperature on the flow boiling heat transfer coefficient of Al_2O_3-water/glycerol nanofluids.

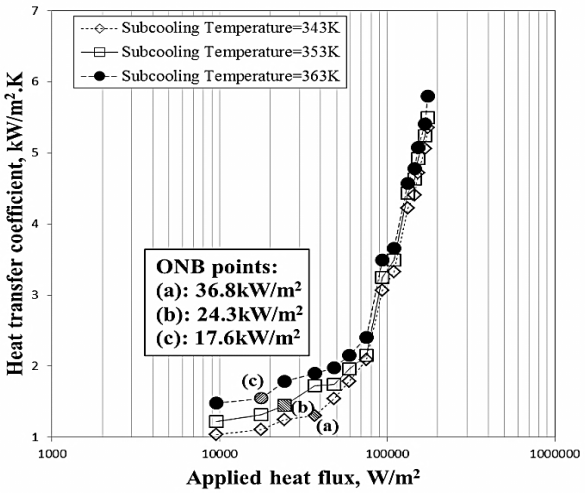

Fig. 11. Effect of sub-cooling temperature on the flow boiling heat transfer of the Al_2O_3-water/glycerol nanofluid

CONCLUSION

A large number of experiments were performed on the convective boiling heat transfer of Al_2O_3-water/glycerol nanofluids at different operating parameters and the following conclusions were drawn:

- Similar to previous studies, two significant heat transfer regions with different heat transfer mechanisms were observed, namely: forced convective and nucleate boiling.
- Investigations on the operating parameters indicated that both heat flux and mass flux had a direct influence on the heat transfer coefficient and the fouling resistance. On increasing the heat and mass fluxes, the heat transfer coefficient increases in both regions.
- On increasing the concentration of nanofluids, deterioration of heat transfer coefficients can be seen which is due to the deposition of nanoparticles on the heating surface.
- The only influence of sub-cooling temperature is to decrease the corresponding heat flux related to the onset of nucleate boiling. In fact, the higher the sub-cooling temperature, the lower corresponding heat flux related to ONB point is reported.
- Nanoparticles deposition can increase the flow pressure drop which was not studied in this work. It is recommended to conduct future research on the possible pressure drop of nanofluids in convective boiling heat transfer.

Acknowledgement: *The authors wish to dedicate this article to Imam Mahdi and appreciate for the financial support by Semnan University.*

NOMENCLATURE

A	area, m^2
b	distance, m
C_p	heat capacity, $J.kg^{-1}.{}^oC^{-1}$
d_h	hydraulic diameter, m
h	enthalpy, J. kg^{-1}
k	thermal conductivity, $W.m^{-1}.{}^oC^{-1}$
L	heater length, m
P	pressure, Pa
q	heat, W
s	distance, m
T	temperature, K
	Subscripts-Superscripts
b	bulk
bs	base fluid
nf	nanofluid
c	critical
fb	flow boiling
in	inlet
out	outlet
l	liquid
m	mixture
n	number of components
nb	nucleate boiling
ONB	onset of nucleate boiling
Sat	saturated
th	thermometers
v	vapor
w	Wall
	Greek symbols
α	heat transfer coefficient, $W.m^{-2}.K^{-1}$
ρ	density, $kg.m^{-3}$
μ	viscosity, $kg.m^{-1}.s^{-1}$
ϕ	Volume fraction

REFERENCES

1. T. Lee, J. H. Lee, Y. H. Jeong, *Int. J. Heat Mass Trans.* **56** 101, (2013).
2. L. Cheng, L. Liu, *Int. J. Refrigeration* **36**, 421, (2013).
3. S.U.S. Choi, Z.G. Zhang, W. Yu, F.E. Lockwood, E.A. Grulke, *Appl. Phys. Lett.*, **79**, 2252, (2001).
4. S.K. Das, N. Putra, W. Roetzel, *Int. J. Heat Mass Trans.*, **46**, 851, (2003).
5. Y. Ding, H. Alias, D. Wen, R.A. Williams, *Int. J. Heat Mass Trans.*, **49**, 240, (2006).
6. M.M. Sarafraz, F. Hormozi, *Exp. Therm. Fluid Sci..*, **52**, 205, (2014).
7. M.M. Sarafraz, F. Hormozi, *Int. Commun. Heat Mass Trans..*, **53**, 116, (2014).
8. D. Wen, Y. Ding, *J. Nanoparticle Res.*, **7**, 265, (2005).
9. H. Kim, J. Kim, M.H. Kim, *Int. J. Heat Mass Trans.*, **49**, 5070, (2006).
10. S.J. Kim, I.C. Bang, J. Buongiorno, L.W. Hu, *Appl. Phys. Lett.*, **89**, 153, (2006)
11. H.D. Kim, J.B. Kim, M.H. Kim, *Int. J. Multiphase Flow*, **33**, 691, (2007).
12. S.J. Kim, I.C. Bang, J. Buongiorno, L.W. Hu, *Bull Polish Academy Sci. Tech. Sci*., **55,** 211, (2007).
13. M.M. Sarafraz, S.M. Peyghambarzadeh, *Exp. Therm. Fluid Sci.*, **50**, *154*, (2013).
14. T.I. Kim, Y.H. Jeong, S.H. Chang, *Int. J. Heat Mass Trans.*, **53**, 1015, (2010).
15. D.C. Groeneveld et al., *Nucl Eng.*, **163**, 1, (1996).
16. Y.H. Jeong, M.S. Sarwar, S.H. Chang, *Int. J. Heat Mass Trans.*, **51**, 1913, (2008)
17. Y.H. Jeong, W.J. Chang, S.H. Chang, *Int. J. Heat Mass Trans.*, **51,** 3025, (2008).
18. J. Lee, Y.H. Jeong, *Nucl. Eng. Des*., **240**, 3594, (2010)
19. G.P. Celata, K. Mishima, G. Zummo, *Int. J. Heat Mass Trans.*, **44**, 4323, (2001).
20. Henderson K, Park YG, Liu L, Jacobi AM. *Int. J. Heat Mass Trans*., **5**, 944, (2010).
21. E. A. H. Abdel-Hadi, S. H. Taher, A. M. Torki, S. S. Hamad, *International Conference on Advanced Materials Engineering*, **15**, 80, (2011).

22. R. Saidur, K.Y. Leong, H.A. Mohammad, *Renewable Sustainable Energy Rev.* **15** 1646, (2011).
23. J. F. Seara, F. J. Uhia, J. Sieres, *Exp. Heat Trans.*, **20**, 123, (2007).
24. S. J. Kline, F.A. McClintock, *Mech. Eng.*, **75**, 3, (1953).

КАЧЕСТВЕНО ИЗСЛЕДВАНЕ НА КОНВЕКТИВНОТО ТОПЛОПРЕНАСЯНЕ С КИПЕНЕ В РАЗРЕДЕНИ СУСПЕНЗИИ НА AL_2O_3 ВЪВ ВОДНО-ГЛИЦЕРОЛОВИ СМЕСИ ВЪВ ВЕРТИКАЛНО ПРЪСТЕНОВИДНО ПРОСТРАНСТВО

М.М. Сарафраз [*], Ф. Хормози

Факултет по химично, нефтено и газово инженерство, Университет Семнан, Иран

Постъпила на 18 юли, 2013 г.; коригирана на 22 февруари, 2014 г.

(Резюме)

Експериментално е изследвано топлопренасянето и е определен коефициента на топлопренасяне при кипене на суспензии от наночастици на Al_2O_3 във водно-глицеролови смеси при различни работни условия. Влиянието на различни работни параметри като топлинния поток, масовия поток и температурата на охлаждане, както и концентрацията на наночастици върху коефициента на топлообмен е изследвано и обсъдено. Резултатите показват, че са налице две различни области на топлопренасяне на конвективен пренос с различни механизми на преносния процес: принудени конвекции в една фаза и дву-фазно кипене със зародишообразуване. Резултатите показват също така, че коефициентът на топлопренасяне нараства с нарастване на топлинния и масовия поток, докато той намалява с нарастване концентрацията на наночастиците. Това се обяснява с отлагането на наночастици върху топлообменната повърхност. Температурата на охлаждане влияе единствено върху възникването на зародиши на кипене.